Glycobiology, 2017, vol. 27, no. 7, 625–634
doi: 10.1093/glycob/cwx031
Advance Access Publication Date: 10 May 2017
Original Article

Analytical Glycobiology

Exploring the structure of fucosylated chondroitin sulfate through bottom-up nuclear magnetic resonance and electrospray ionization-high-resolution mass spectrometry approaches

Gustavo RC Santos, Ana CO Porto, Paulo AG Soares, Eduardo Vilanova, and Paulo AS Mourão[1]

Programa de Glicobiologia, Instituto de Bioquímica Médica Leopoldo de Meis, and Laboratório de Tecido Conjuntivo, Hospital Universitário Clementino Fraga Filho, Universidade Federal do Rio de Janeiro, Rio de Janeiro, RJ 21941-913, Brazil

[1]To whom correspondence should be addressed: Tel: +55-21-3938-2090; Fax: +55-21-3938-2090; e-mail: pmourao@hucff.ufrj.br.

Received 3 March 2017; Revised 5 April 2017; Editorial decision 9 April 2017; Accepted 18 April 2017

Abstract

Fucosylated chondroitin sulfate (FCS) from sea cucumbers is composed of a chondroitin sulfate (CS) central core and branches of sulfated fucose. The structure of this complex glycosaminoglycan is usually investigated via nuclear magnetic resonance (NMR) analyses of the intact molecule, ergo through a top-down approach, which often yield spectra with intricate sets of signals. Here we employed a bottom-up approach to analyze the FCSs from the sea cucumbers *Isostichopus badionotus* and *Ludwigothurea grisea* from their basic constituents, viz. CS cores and sulfated fucose branches, obtained via systematic fragmentation through mild acid hydrolysis. Oligosaccharides derived from the central CS core were analyzed via NMR spectroscopy and the disaccharides produced using chondroitin sulfate lyase via SAX-HPLC. The CS cores from the two species were similar, showing only slight differences in the proportions of 4- or 6-monosulfated and 4,6-disulfated β-D-GalNAc. Sulfated fucose units released from the FCSs were analyzed via NMR and ESI-HRMS spectroscopies. The fucose units from each species presented extensive qualitative differences, but quantitative assessments of these units were hindered, mostly because of their extensive desulfation during the hydrolysis. The bottom-up analysis performed here has proved useful to explore the structure of FCS through a sum-of-the-parts approach in a qualitative manner. We further demonstrate that under specific acidification conditions particular fucose branches can be removed preferentially from FCS. Preparation of derivatives enriched with particular fucose branches could be useful for studies on "structure vs. biological function" of FCS.

Key words: Glycosaminoglycans, marine invertebrate, polysaccharide fragmentation, preparation of oligosaccharides, sea cucumber

Introduction

Fucosylated chondroitin sulfate (FCS) is a unique natural glycosaminoglycan (GAG) found in the extracellular matrix of the body wall of sea cucumbers (Vieira and Mourão 1988). This polysaccharide consists of a chondroitin sulfate (CS) central core composed of alternating β-D-glucuronic acid and *N*-acetyl-β-D-galactosamine

disaccharide building blocks and branches of sulfated α-L-fucose linked to position 3 of glucuronic acid units of the CS core (Santos et al. 2015). The presence of sulfated fucose branches gives to FCS therapeutic properties in a range of pathological and physiological systems (e.g., coagulation, inflammation, cancer) that are not seen in non-fucosylated CS from vertebrates and other invertebrates (Borsig et al. 2007; Fonseca et al. 2010; Melo-Filho et al. 2010; Huang et al. 2013; Liu et al. 2016a; Marques et al. 2016).

Investigations correlating physiological functions or pharmacological properties of GAGs with their chemical structures are mostly performed using modified derivatives obtained through: (1) enzymatic cleavage (GAG lyases) or specific chemical degradations yielding oligosaccharides with well-defined structure; (2) chemical modifications such as desulfation, oversulfation and carboxyl-reduction and (3) under- or overexpressing enzymes related to the synthesis of the GAGs using modified animals or cells. Comparing the activities of modified and non-modified GAGs makes it possible to determine the specific epitopes involved in a given biological or pathological system (Gandhi and Mancera 2008).

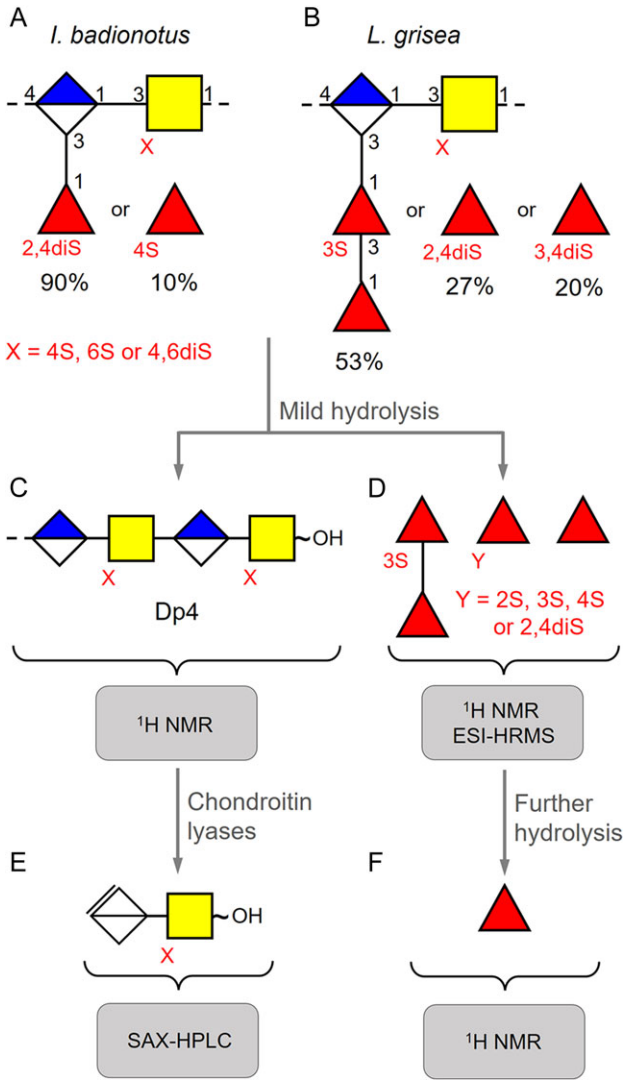

Fig. 1. Diagram of the proposed structure of FucCS from the sea cucumbers *I. badionotis* (**A**) and *L. grisea* (**B**) and their fragments obtained through mild acid hydrolysis (**C, D** and **F**) and digestion with chondroitin ABC lyase (**E**). The methods used for analysis of the fragments are specified in the gray boxes. This figure is available in black and white in print and in colour at *Glycobiology* online.

Except for generic chemical reactions of defucosylation, desulfation and carboxyl-reduction, the other methodologies customarily employed to produce derivatives of GAGs with specific and well-determined structural modifications are unfeasible to modify FCS. The presence of fucosylated branches inhibits the enzymatic cleavage of FCS using CS lyases or hydrolases; furthermore, chemical degradation methods to produce FCS oligosaccharides with well-defined structure have not been consolidated yet (Wu et al. 2013; Gao et al. 2015; Yang et al. 2015; Li et al. 2016). Structural modifications of FCS via alterations on its biosynthetic pathways are also unfeasible because the enzymes involved in the fucosylation of the CS core as well as their related genes are still far from being determined (Laezza et al. 2016; Vinnitskiy et al. 2017).

FCSs of several species of sea cucumbers have already been described using analytical tools such as nuclear magnetic resonance (NMR) spectroscopy, mass spectroscopy (GC/LC–MS) and infrared spectroscopy (FT-IR) (Myron et al. 2014). These polysaccharides allegedly present similar CS central cores composed for β-D-glucuronic acid 1→3 *N*-acetyl-β-D-galactosamine, in spite of the uncertain sulfation position in the galactosamine units (Santos et al. 2015) However, the α-L-fucose branches 3-linked to the glucuronic acid units of the CS core structurally differ in a species-specific manner in both their sizes (mono- or difucosylated) and patterns of sulfation (Chen et al. 2010; Myron et al. 2014).

Most of the structural analyses of FCSs are carried out based on extensive sets of 1D and 2D NMR spectra of their intact polymers (Santos et al. 2015), ergo through a "top-down" approach, in which important molecular aspects such as fucosylation and sulfation patterns are analyzed all at once (Cegelski 2015). The problem with this approach is that these NMR spectra often present an intricate set of signals with difficult assignment and hence are susceptible to misinterpretations (Santos et al. 2015). An option to avoid these complex NMR interpretations is employing a "bottom-up" analytical strategy, where the components of FCS (fucose branches and CS disaccharides) are analyzed separately and then assembled together through a "sum-of-the-parts" approach (Cegelski 2015). However, the feasibility of bottom-up analyses of FCSs relies on developing a methodology for their systematic fragmentation, which yields mono- or oligosaccharides with simple structures and easier interpretation.

In the present study, we proceed with the systematic fragmentation and bottom-up analysis of FCSs from the sea cucumbers *Isostichopus badionotus* and *Ludwigothurea grisea*. The FCSs from these species were selected because they have well-defined structures, which consist of similar CS central cores but markedly different fucose branches: *I. badionotus* presents relatively simple branches (Figure 1A) composed of monofucosylated units mostly 2,4-disulfated and in a minor extent 4-sulfated (Santos et al. 2015) while *L. grisea* presents intricate composition of branches (Figure 1B) including 3-sulfated difucosylated units and 2,4-disulfated and 3,4-disulfated monofucosylated units (Santos et al. 2015). Initially, we submitted these FCSs to mild acid hydrolysis to detach the fucose branches from the CS central cores. The fucoses released from the branches were characterized via NMR and electrospray ionization-high-resolution mass spectrometry (ESI-HRMS) (Figure 1D and F) and the CS cores via NMR and their disaccharides produced by enzymatic cleavage (chondroitin lyases) via anion-exchange chromatography (Figure 1C and E). The bottom-up approach employed here is an important analytical tool for determining the fine structure of complex sulfated polysaccharides, an essential feature to

support studies correlating the structure of these molecules and their biological activities.

Results and discussion

Central core of FCS

Glycosidic linkages between galactosamine and glucuronic acid of the CS central cores of FCSs are much less labile in acid conditions than those between the fucose units of branches, which makes this GAG particularly suitable for fragmentation by mild acid hydrolysis (Mourão et al. 1996). This approach has already been used to remove fucose branches from the central core of FCS, yielding intact CS chains (Mourão et al. 1996; Liu et al. 2016b). Here we submitted the FCSs from the sea cucumbers *I. badionotus* and *L. grisea* to mild acid hydrolysis with 0.15 M H_2SO_4 at 100°C for 45 min and then separated the formed products using gel permeation chromatography. This hydrolysis condition assures a complete defucosylation of the CS core and was established after testing several different reaction times and temperatures (not shown). The major hydrolysis products were sulfated fucoses released from the branches, and a series of oligosaccharides (Dp4 → Dp8) derived from the CS core (Figure 2A). The presence of hexuronic acid (not shown) in these oligosaccharides confirms that they derived from the CS core.

Oligosaccharides Dp4 → Dp8 derived from the FCSs of both species were subsequently analyzed via 1D ^{1}H NMR spectroscopy. Signals referent to the α-fucose units (Fuc-CH_3 at ~1.35 ppm) decreased drastically in the spectra; notwithstanding, the signals from the CH_3 of the *N*-acetyl-β-D-galactosamine units (GalNAc-CH_3 at ~2.12 ppm) remains unchanged after the hydrolysis (Figure 2B). Anomeric signals from β-D-glucuronic acid and *N*-acetyl-β-D-galactosamine units are tough to identify on 1D ^{1}H spectra because they superimposed with the water signal (Santos et al. 2015). However, the α-anomeric signals from these two units after mutarotation equilibrium were clearly identified at ~5.25 ppm as an undistinguishable peak and their intensities increase as their molecular weight decreases (Dp8 < Dp6 < Dp4), as expected (Figure 2B).

Analysis of the oligosaccharides (Dp4 → Dp8) derived from the FCS central core via 2D NMR revealed that Dp8 and Dp6 have more complex spectra than DP4, which yields relatively simple spectra (Figure 2C and D). No difference was observed between the spectra of Dp-4 from the two species. Five distinct spin systems were identified on the ^{1}H–^{1}H TOCSY spectrum of Dp-4. Two of them were attributed to internal units of β-D-glucuronic acid and of *N*-acetyl-β-D-galactosamine (Figure 2C and D, solid line rectangles) and the other three to reducing end units formed after mutarotation equilibrium of α/β-glucuronic acid and *N*-acetyl-α-galactosamine (Figure 2C and D, dashed line rectangles). The system attributed to the reducing end *N*-acetyl-β-D-galactosamine was difficult to visualize due to its overlapping with the water signal. The chemical shifts of these five spin systems are available in the Supplementary data, Tables S1 and S2 and are in strictly accordance with data obtained from other CSs published elsewhere (Neville et al. 1989; Sugahara et al. 1996).

Reducing end units of *N*-acetyl galactosamine are preponderant over those related to terminal glucuronic acid. This is clearly demonstrated comparing the integrals of H3 signals from reducing end α-D-glucuronic acid vs. *N*-acetyl-α-D-galactosamine units and from reducing end vs. internal units of β-glucuronic acid (Supplementary data, Table S3). This preponderance of *N*-acetyl-galactosamine in the reducing terminal indicates that the acid mild hydrolysis favors the cleavage of galactosaminyl instead of glucuronyl linkages.

The strong downfield shift observed in the H4 signal from the *N*-acetyl galactosamine, resonating at ~4.80 ppm (Figure 2C and D), indicates a 4-sulfation of this unit. Sulfation at position 6 of *N*-acetyl galactosamine is tough to assign based only on the ^{1}H–^{1}H TOCSY spectrum. Therefore, to assure a thorough analysis of the sulfation pattern of the CS cores of each species we performed an enzymatic cleavage of the oligosaccharides (Dp4 → Dp8) with chondroitin ABC lyase and then analyzed the disaccharides formed using a SAX column linked to a HPLC system (Figure 3). Both species presented 4-, 6-sulfated and 4,6-disulfated *N*-acetyl-β-D-galactosamine units though with different proportions: CS core from *L. grisea* had preponderantly 4-sulfated and 4,6-disulfated units while 6-sulfated units were more abundant in the CS core from *I. badionotus* (Supplementary data, Table S4). No sulfation was detected on the β-D-glucuronic acid units. We also attempted to analysis Dp-4 → Dp-8 through ESI-MS but the extensive desulfation did not allow a clear interpretation of the spectra.

CS central cores of FCSs from several species of sea cucumbers have been mostly described as disaccharide repetitive units of β-D-glucuronic acid and *N*-acetyl-β-D-galactosamine sulfated at position 4- and/or 6- (Myron et al. 2014). Using the approach depicted on panels C and E of Figure 1, we demonstrated that the sulfation at position 4- but not at position 6- of the galactosamines are assignable on ^{1}H–^{1}H TOCSY spectra and hence a precise determination of the sulfation patterns of these units were only possible through the analyses of disaccharides generated by enzymatic cleavage of Dp4 → Dp8 oligosaccharides. The SAX-HPLC analyses of these disaccharides clearly showed that the CS cores from both species are similar to the chondroitin sulfate type E (CS-E) from mollusks, which consist of β-D-GlcA 1→3 linked to units of non-sulfated, 4- or 6-monosulfated or 4,6-disulfated β-D-GalNAc (Bergefall et al. 2005; Jinno-Oue et al. 2013). The only difference detected between these CS cores was in the proportions of the different sulfated β-D-GalNAc units (Supplementary data, Table S4), as observed for the FCS from the species *Cucumaria frondosa* and *Thelenota ananas* (Liu et al. 2016b).

Fucose branches of FCS

The mixtures of sulfated fucoses removed from the FCSs through mild hydrolysis with H_2SO_4 and isolated via gel permeation chromatography (Figure 2A) were initially analyzed via 1D ^{1}H (Figure 4A and B), 2D ^{1}H–^{1}H COSY (not shown) and ^{1}H–^{1}H TOCSY NMR spectra (Supplementary data, Figure S1). We identified several spin systems (five for *L. grisea* and four for *I. badionotus*) ascribed to fucose with distinct sulfation patterns. H4 of 4-sulfated units resonates in the same region of the spectra as the β-anomeric protons, but these signals were discernible due to the typically large $^3J_{H1\text{-}H2}$ of the β-anomers (~4 and ~8 Hz for the α- and β-anomers, respectively) (Santos et al. 2015). Moreover, the characteristic ~6 ppm downshift of the proton signals at the sulfation site allows determining the sulfation patterns of the fucose units (Supplementary data, Table S5). ^{1}H–^{13}C HSQC analyses of the mixtures of sulfated fucose yielded spectra with poor resolution due to scarcity of material (data not shown); notwithstanding, some discernible signals confirmed the assignments obtained by the ^{1}H–^{1}H spectra.

The FCS from each species of sea cucumber yields different proportions and types of fucose units (Table I). We determined these

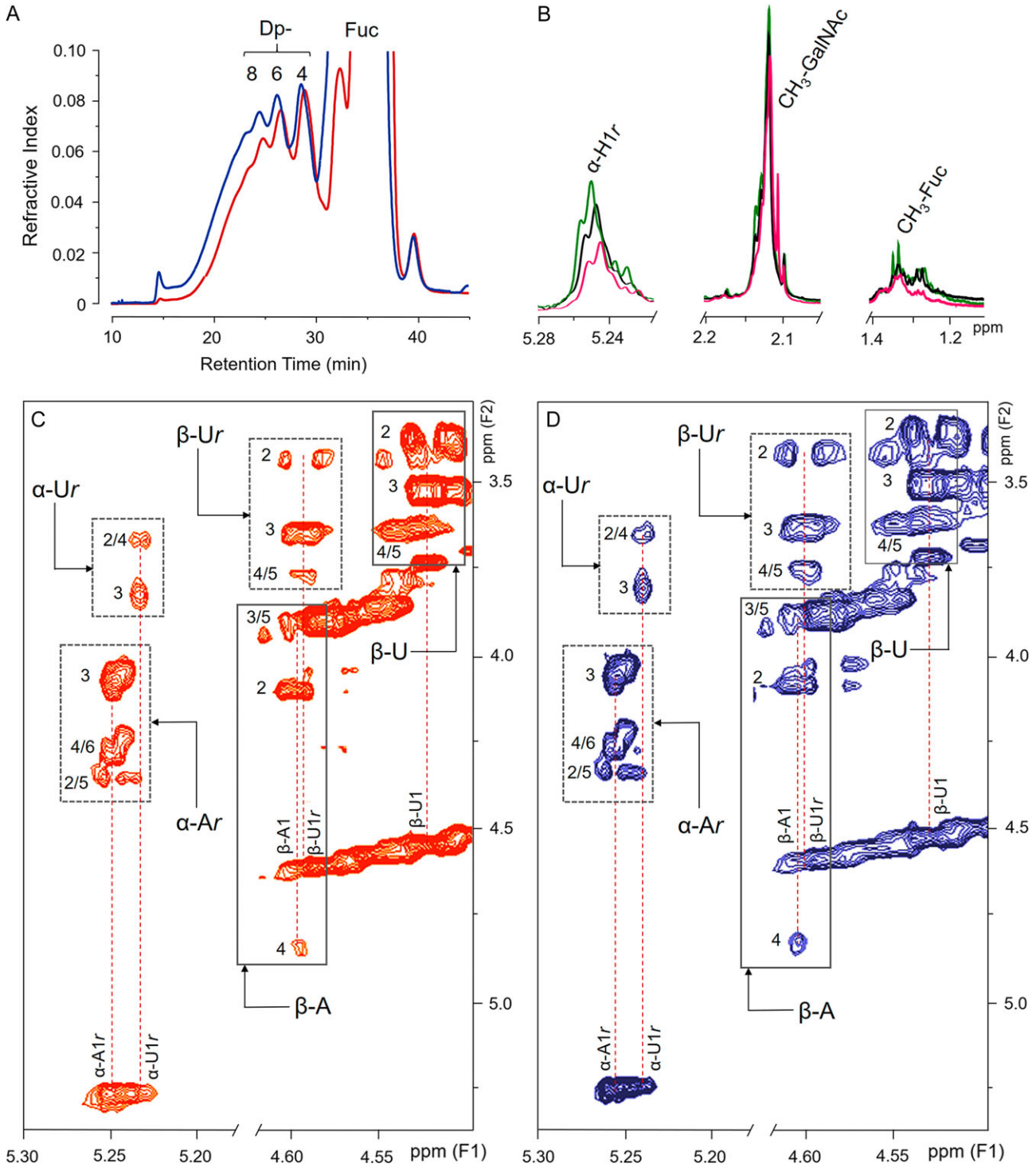

Fig. 2. Preparation and analysis of oligosaccharides derived from the central CS core of FucCS. (**A**) Gel permeation chromatography of the products formed by mild acid hydrolysis. Fractions containing the tetra (Dp-4), hexa (Dp-6), octasaccharide (Dp-8) and the fucose mixture were pooled and lyophilized. (**B**) Expansions of the 1D ^{1}H NMR spectra of Dp-4 (in green), Dp-6 (in black) and DP-8 (in purple), α-H1*r* refers to the anomeric signals of free reducing terminal of α-D-glucuronic acid and of *N*-acetyl-α-D-galactosamine. Expansion of the ^{1}H–^{1}H TOCSY of Dp-4 obtained from FucCS of *I. badionotus* (C, in red) and *L. grisea* (D, in blue). U and A refer to signals from glucuronic acid and *N*-acetyl-galactosamine, respectively. Solid line and dashed line rectangles indicate the spin systems of internal units and of reducing end (*r*) residues, respectively. This figure is available in black and white in print and in colour at *Glycobiology* online.

proportions with basis on the α-anomers signals in order to avoid interference of H4 of 4-sulfated units. As described before (Santos et al. 2015), fucose 2,4-disulfated preponderates in the FCS of *I. badionotus* while fucose 3-sulfate occurs only in the FCS from *L. grisea* (Table I). Comparison between the proportions of fucose derivatives obtained through mild hydrolysis with predictable values

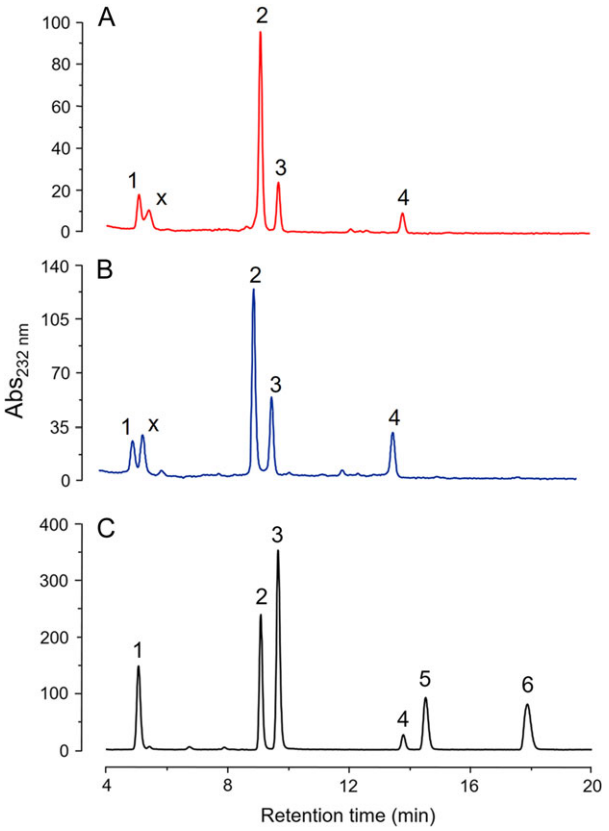

Fig. 3. Analyses of disaccharides via SAX-HPLC. Analyses of disaccharides produced through enzymatic cleavage with chondroitin ABC lyase of Dp-4 → Dp-8 oligosaccharides of FucCSs from (**A**) *I. badionotus*, (**B**) *L. grisea* and (**C**) CS disaccharide standards. The numbered peaks correspond to the elution positions of the CS disaccharide standards as follows: peak 1, ΔGlcUA-GalNAc; peak 2, ΔGlcUA-GalNAc6S; peak 3, ΔGlcUA-GalNAc4S; peak 4, ΔGlcUA-GalNAc4,6S; peak 5, ΔGlcUA2S-GalNAc4S; peal 6, ΔGlcUA2S-GalNAc4,6diS. This figure is available in black and white in print and in colour at *Glycobiology* online.

based on NMR analysis of intact FCSs (Santos et al. 2015) showed discrepancies, especially the lower proportions of disulfated fucose (either 2,4- or 3,4-disulfated) and higher proportions of monosulfated and/or nonsulfated derivatives (Table I). Such differences indicate that the fucose from the branches undergoes to desulfation either before or after their removal from the central CS core during the acidification reaction. Further hydrolysis of the fucose mixtures showed a drastic decrease of the sulfated derivatives in the time course of reaction, up to an extent that non-sulfated fucose became predominant in the mixtures (Supplementary data, Figure S2).

Since the hydrolysis of FCS using H_2SO_4, even in mild conditions, induces desulfation of the fucose units from the branches, we employed an alternative methodology aiming for a milder hydrolysis of the FCSs using the ion exchange resin Dowex H^+. This approach consists in a very mild acidification of the reaction solution and does not require further desalting or gel permeation chromatographic steps. 1D ^1H and 2D ^1H–^1H TOCSY spectra (not shown) of the fucose mixtures hydrolyzed using Dowex H^+ revealed that this method produces the same types of derivatives but with slightly different proportions; notably, the proportions of 2,4-disulfated fucose were higher than those obtained through hydrolysis using H_2SO_4 (Table I). Fucose 3,4-disulfated found in the branches of the FCS from *L. grisea* seems particularly labile to hydrolysis because it is not found in the hydrolysates produced using both H_2SO_4 or Dowex H^+. Nevertheless, the mild hydrolysis using Dowex H^+ still desulfating the fucose units in a non-specific manner (Table I) and thus do not bring a relevant advantage over traditional acid hydrolysis methods.

In addition to the 1D and 2D NMR spectroscopy, we also analyzed the fucose mixtures obtained via high-resolution mass spectrometry by determining the experimental masses of precursor (ESI-MS) and product (ESI-MS/MS) ions of the different sulfated fucose units (Supplementary data, Table S6). ESI-MS spectra of the fucose mixture from *L. grisea* (Figure 4C) and *I. badionotus* (not shown) were remarkably similar and generate a preponderant mass corresponding to monosulfated fucose (m/z = 243.0177) and small amounts of disulfated fucose (Figure 4C). Surprisingly, a trace amount of monosulfated fucose disaccharides, undetectable in the NMR spectra, was detected in the ESI-MS spectra (Figure 4C, inset). Free sulfate observed in the spectra indicates that some desulfation may occur during the ESI-MS analysis, which possibly accounts for the low content of disulfated fucose in the mixture.

The product ions of monosulfated fucose (m/z = 243.0177) were then analyzed via ESI-MS/MS (Figure 4D) and confirmed the presence of fucose 2-sulfate. Fucose 3- or 4-sulfate also occur in the mixtures but it is not possible to distinguish these two isomers since they yield similar product ions (Daniel et al. 2007). Free sulfate was also detected on the ESI-MS/MS indicating further desulfation during the fragmentation. Therefore, high-resolution mass spectrometry was useful as a complementary methodology to confirm qualitative NMR data, mostly by detecting monosulfated fucose disaccharides; however, it was inappropriate for quantitative determinations, especially due to the extensive desulfation of the fucose units during spectra aquisition.

Analyses of the fucose mixtures obtained through mild acid hydrolysis via NMR and ESI-HRMS were proven appropriate for qualitative assessments of the fucose branches found in the different FCSs. Fucose 2,4-disulfated occur in higher and non-sulfated fucose in lower proportions in the hydrolysates obtained from *I. badionotus* than in those obtained from *L. grisea*; these differences reflect the distinct sulfation pattern of the fucose branches of the FCSs from different species of sea cucumber (Chen et al. 2010; Santos et al. 2015; Liu et al. 2016b). However, we cannot obtain reliable quantitative information on the proportions of the different sulfated fucose units through these approaches mainly due to extensive desulfation during the hydrolysis reactions with both H_2SO_4 and Dowex H^+ and the ionization steps of the ESI-HRMS assays. Beside these quantitative inaccuracies, the analysis via ESI-HRMS also showed qualitative limitations, this is because the spectra of the fucose mixtures from the two species were strikingly similar and also by the inability of the technique to distinguish fucose 3-sulfate from fucose 4-sulfate.

Defucosylation vs. desulfation during hydrolysis of FCS

The condition of the mild acid hydrolysis (0.15 M H_2SO_4, at 100°C for 45 min) employed here was set to assure a complete removal of fucose branches from the FCSs. Although this is an optimal condition for an appropriate analysis of the central CS core, it causes extensive desulfation of the fucose units from the branches. Therefore, establish the equilibrium between defucosylation and desulfation during mild acid hydrolysis is necessary to enhance the quantitative assessments of the sulfated fucose units released from

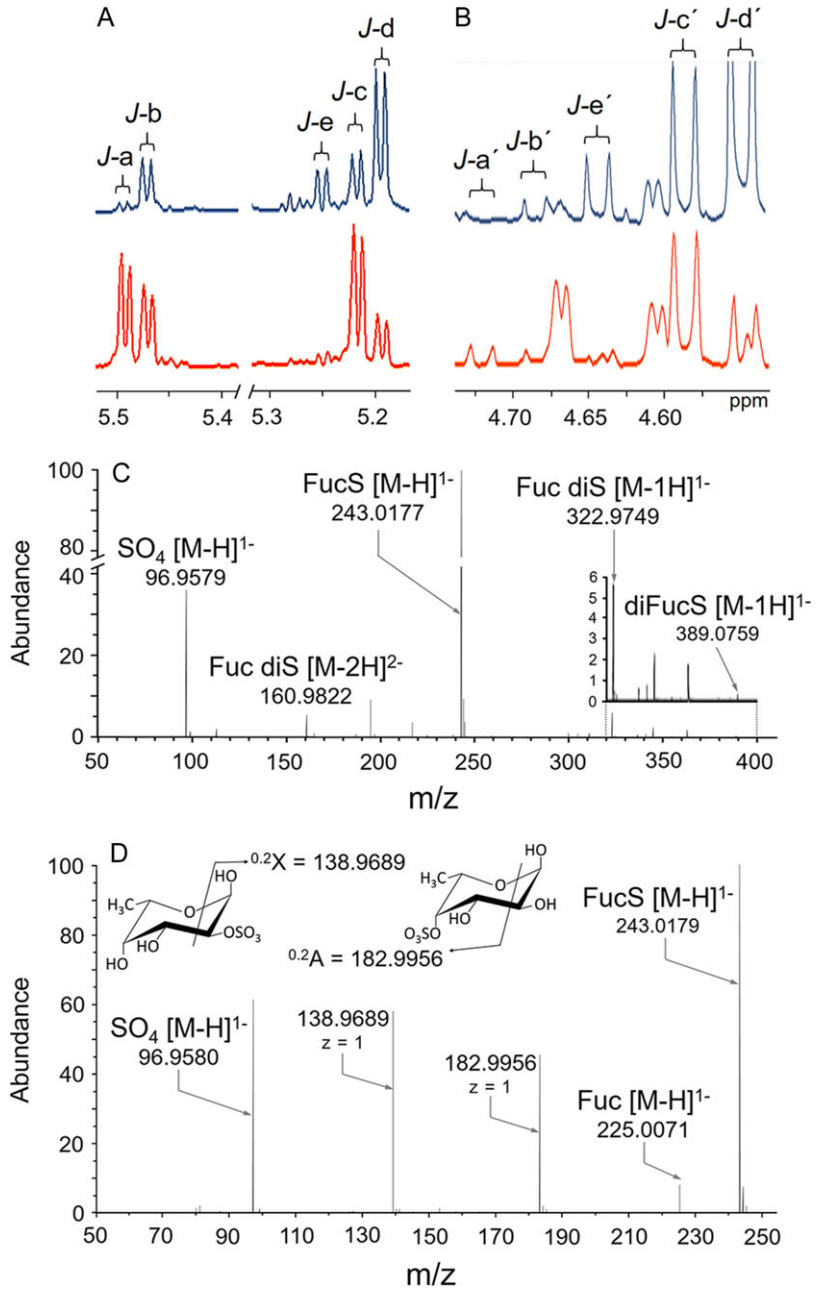

Fig. 4. Analysis of the fucose mixtures produced through mild acid hydrolysis. (**A** and **B**) Fucose mixtures obtained from the FucCSs of *I. badionotus* (in red) and *L. grisea* (in blue) were analyzed via 1D ^{1}H NMR spectrometry. Protons of α- and β-anomers of: a, fucose 2,4-disulfate; b, fucose 2-sulfate; c, fucose 4-sulfate, d, fucose non-sulfated and e, fucose 3-sulfate. *J* represents $^{3}J_{H1\text{-}H2}$ in Hz. See also Supplementary data, Fig. S2 for the assignments of these signals. (**C**) ESI-MS of the fucose mixture from *L. grisea* obtained through mild acid hydrolysis. The inset shows an expansion of the 320–400 *m/z* region. (**D**): ESI-MS/MS of the product ions from fucose monosulfate (*m/z* 243.0177). This figure is available in black and white in print and in colour at *Glycobiology* online.

the CS core and thus improve the determination of FCSs structures through a bottom-up approach.

In order to investigate the equilibrium between defucosylation and desulfation, we subjected the FCSs from the two species to acid hydrolysis in milder conditions (0.5 M HCl, 50°C) and followed the reactions via 1D ^{1}H NMR real-time reaction monitoring (Kamba et al. 2016) (Figure 5). The FCS from *I. badionotus* presents a simple composition of fucose branches (Santos et al. 2015) (Figure 1A) and thus the changes in the ^{1}H NMR spectra in the time course of the reaction were easily interpreted (Figure 5A). The major modifications observed were a decrease of the anomeric signal of α-fucose 2,4-disulfate linked to the CS core (signal I at 5.70 ppm) and the parallel increase of three sets of signals. Two of them were assigned to free fucoses released from the CS core, as indicated by doublets with $^{3}J_{H1\text{-}H2}$ ~3.8 Hz, ascribed to α-fucose 2,4-disulfate and α-fucose 4-sulfate (signals II and IV at 5.50 and 5.22 ppm). The third signal represents the anomeric proton of α-fucose 4-sulfate that still linked to the central core (signal III at 5.45 ppm). Nonsulfated fucose, either linked to the core or free in solution, is not formed. We estimated a decrease of 53.6% of 2,4-disulfated

Table I. Comparison between the proportions of the different types of fucose units in FCSs (% of total) as predict and effectively found after mild acid hydrolysis

Species	Type of fucose unit	Predict[a]	Observed after mild hydrolysis[b]	
			H_2SO_4	Dowex H^+
I. badionotus	Fuc-2,4diSO$_4$	90	30 (–60)[c]	37 (–53)
	Fuc 4SO$_4$	10	35 (+25)	35 (+25)
	Fuc-3SO$_4$	<1	<1	<1
	Fuc-2SO$_4$	<1	20 (+20)	19 (+ 19)
	Fuc	<1	16 (+16)	9 (+9)
L. grisea	Fuc-2,4diSO$_4$	18	1 (–17)	9 (–9)
	Fuc-3,4diSO$_4$	12	<1 (–12)	<1 (–12)
	Fuc-3SO$_4$	35	24 (–11)	8 (–27)
	Fuc	35	46 (+11)	70 (+35)
	Fuc-4SO$_4$	<1	14 (+14)	6 (+6)
	Fuc-2SO$_4$	<1	15 (+15)	7 (+7)

[a]Based on NMR analysis of intact FCS (Santos et al., 2015).
[b]Based on the integrals of the α-anomers (see Figure 4A).
[c]Increased (+) or decreased (–) proportions (%) of the fucose units observed on the acid hydrolysates compared with the predict values.

fucose branches during the 5 h-hydrolysis period with basis on the decrease of signal I (Figure 5A).

Certainly, the intensity of NMR signals in Figure 5A cannot be compared quantitatively because free fucose mutarotate in solution and only the α-anomers are seen in Figure 5A; furthermore, relaxation properties of spins of sugars free in solution and linked to polysaccharide differ. But the syncronization among signals shifting their intensities during the course of the mild hydrolysis indicate that cleavage of the α-fucosyl linkage (yielding products II and IV) and desulfation (originating signal III) occur simultaneously.

The FCS from *L. grisea* presents a much more complex set of fucose branches than that from *I. badionotus* (Santos et al. 2015) (Figure 1A and B). Even so, both polysaccharides showed some similar modifications during the time course of the hydrolysis; notably, the anomeric signal of fucose 2,4-disulfate linked to the CS core (signal I) decreases and the signal from free fucose 2,4-disulfate and/or fucose 2-sulfate (signal II) increases (Figure 5B). In addition to these coincident modifications, we also observed a marked decrease in the signal of fucose 3-sulfate from the reducing end of the difucosylated branches (signal V at 5.42 ppm); in parallel, we noticed a change in the 5.26–5.32 ppm (signal VI) region of the spectra, possibly as a consequence of the release of these disaccharides (Figure 5B). The up-field shift of ~0.18 ppm from signal V to signal VI is in accordance with the shift expected between 3-sulfated fucose linked and non-linked to the CS core (Santos et al. 2015) (compare data from Supplementary data, Table S5). Moreover, the ESI-HRMS spectra also revealed the release of monosulfated fucose disaccharide with m/z = 389.0758 (Supplementary data, Table S6) during the hydrolysis. Only at longer periods of hydrolysis (>3 h) we observed formation of fucose 3-sulfate and non-sulfated fucose (signals VII and VIII, respectively), possibly denoting the cleavage of the disaccharides (Figure 5B). Finally, we noticed a decrease of the signal IX, assigned to H4 of 4-sulfated units (Figure 5B). With basis on the integrals of signals I and V, we estimated that 5 h-hydrolysis affect 55.3% of 2,4-disulfated fucose and 86.3% of the 3-sulfated disaccharides, respectively. It is difficult to rely on detection of sulfated disaccharide by ESI-MS due to extensive desulfation and cleavage of the glycosidic linkage, as already reported by elsewhere (Daniel et al. 2007).

In recent years, several methods for depolymerization of FCSs including β-elimination, Cu^+ catalytic free-radical reactions, ^{60}Co irradiation and Fenton-system degradation have been developed (Wu et al. 2013; Gao et al. 2015; Yang et al. 2015; Li et al. 2016). However, these methodologies are usually employed to cleave the CS core of the FCSs aiming the production of derivatives with reduced molecular weight (Santos et al. 2015; Panagos et al. 2014); therefore, ergo acid hydrolysis still is the method of choice for defucosylation of FCSs. The 1D ^1H NMR real-time reaction monitoring of the mild hydrolysis of the FCSs from *I. badionotus* and *L. grisea* revealed that both defucosylation and desulfation occur concomitantly. We observed for the FCS of *L. grisea* that fucose disaccharide units are preferentially affected by the acidification than branches of fucose 2,4-disulfate; however, the glycosidic linkage between the fucose units of these disaccharides, even after removal from the CS core, have shown surprisingly resistant to acid hydrolysis. These results suggest that particular fucose branches can be removed preferentially from FCSs through specific acidification conditions. Mild hydrolysis has been using for cleavage of sulfated fucose containing polysaccharides such as linear fucans from sea urchins (Pomin et al. 2005a, 2005b; Queiroz et al. 2015). This reaction yields oligosaccharides with well-defined structure through the selective removing of a 2-sulfate ester followed by the cleavage of the glycosidic linkage between the recently desulfated and the adjacent 4-sulfated units. The cleavage on a precise position of the sulfated fucan chain possibly relates to a sulfate-dependent electrostatic repulsion force and steric hindrance effects (Queiroz et al. 2015).

Conclusions

In the present study, we employed a bottom-up approach (Cegelski 2015) to investigate the structure of FCSs from the sea cucumbers *I. badionotus* and *L. grisea*. The major challenge to perform this approach was to fragment the FCSs into their main components (CS cores and sulfated fucose branches) causing less chemical degradation as possible. After testing several conditions of mild acid hydrolysis we successfully separated the CS cores from the sulfated fucose branches. The CS cores from the two species were similar, showing only slight differences in the proportions of 4- or 6-monosulfated and 4,6-disulfated β-D-GalNAc, but their fucose units released after acidification showed extensive qualitative differences, as previously described for the intact polysaccharides (Santos et al. 2015). However, a quantitative assessment of the different sulfated fucose units was hindered, mostly because of their extensive desulfation during the hydrolysis. Therefore, the bottom-up analysis employed here has proved useful to explore the structure of FCSs through a sum-of-the-parts approach in a qualitative manner. Such qualitative investigations are essential for a precise structural determination of FCSs, especially for those with complex branches composition like that from *L. grisea*, which in turn took almost 20 years to be thoroughly characterized (Mourão et al. 1996). Furthermore, we observed that defucosylation and desulfation occur concomitantly during the hydrolysis and thus under specific acidification conditions particular fucose branches, such as the 3-sulfate fucose disaccharides of *L. grisea*, can be removed preferentially from FCSs. Preparation of FCS derivatives enriched with particular fucose branches could be useful for studies on "structure *vs.* function" in a range of biological and pathological systems.

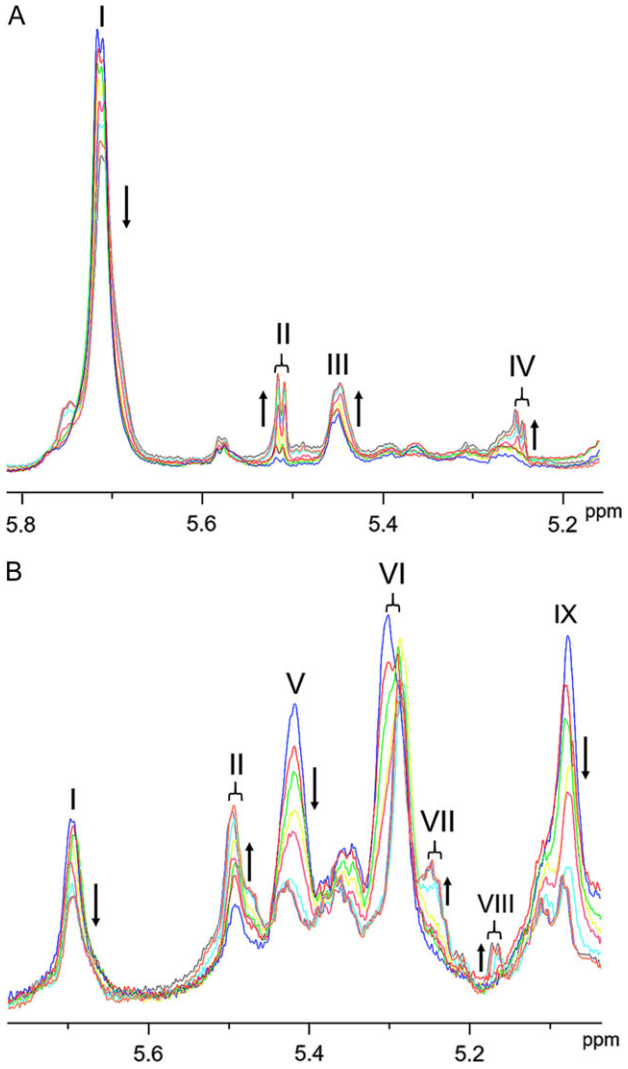

Fig. 5. 1D ^{1}H NMR real-time reaction monitoring of the mild hydrolysis (0.5 M HCl at 50°C) of the FucCSs from *I. badionotus* (**A**) and *L. grisea* (**B**). The reactions were monitored at 0 min (blue), 15 min (red), 30 min (green), 60 min (yellow), 120 min (magenta), 180 min (cyan), 240 min (orange) and 300 min (gray). Roman numbers indicate signals of: anomeric protons from α-fucose 2,4-disulfate linked to the CS core (I); free α-fucose 2,4-disulfate (II); α-fucose 4-sulfate linked to the CS core (III); free α-fucose 4-sulfate (IV); α-fucose 3-sulfate at the reducing end of disaccharides linked to the CS core (V); α-fucose disaccharide released from the core (VI); free α-fucose 3-sulfate (VII); free non-sulfated α-fucose (VIII) and H4 from 4-sulfated fucose units (IX). In the Panel B, signal II may represent α-fucose 2-sulfate, 2,4-disulfate or a mixture of both. Arrows up and arrows down represent increasing and decreasing signals, respectively. Vertical braces depict doublets with $^{3}J_{H1\text{-}H2}$ ~3.8 Hz. Signals were assigned with basis on reference data (Santos et al., 2015) and Supplementary data, Table S5. This figure is available in black and white in print and in colour at *Glycobiology* online.

Materials and methods

Extraction and purification of FCS

The sea cucumbers *I. badionotus* and *L. grisea* were collected at Rio de Janeiro coast, Brazil. FCSs were extracted from the body wall of the specimens through proteolytic digestion and purified via anion exchange chromatography as described elsewhere (Santos et al. 2015). The purity of the samples was checked via 1D ^{1}H NMR spectroscopy.

Fragmentation of FCS components through mild acid hydrolysis

FCS (50 mg from each species) was submitted to mild acid hydrolysis in 1.0 mL of 0.15 M H_2SO_4, at 100°C for 45 min; the reaction was interrupted adjusting the pH to 7.0 with 1.0 M NaOH in ice-cold. The hydrolysates were applied to a Superdex peptide column (GE Healthcare) linked to a HPLC system (Shimadzu) equilibrated with ammonium acetate 0.5 M, pH 5.0 and then eluted at a flow rate of 0.5 mL min^{-1} with the same buffer monitored by refractive index. Fractions containing oligosaccharides originated from the CS core (tetra, hexa and octasaccharides) and a mixture of sulfated fucose released from the core were individually pooled and lyophilized.

Analysis of FCS components via solution NMR

1D and 2D ^{1}H spectra of FCS recorded using a 500 MHz NMR spectrometer (Bruker Biospin, Rheinstetten, Germany) with a triple resonance probe Vilanova et al. (2016). Approximately 5 mg of each sample dissolved in 0.5 mL of 99.9% deuterium oxide (Cambridge Isotope Laboratory, Cambridge, MA). All spectra recorded at 50°C with deuterated water exhibiting a peak due to exchange with residual H_2O (HOD), suppressed by presaturation. For 1D ^{1}H NMR (*zgpr* from Bruker library) spectra, 64 scans were recorded, using an inter-scan delay equals 1 s. 2D ^{1}H–^{1}H COSY (*cosyphpr* from Bruker library) and ^{1}H–^{1}H TOCSY (*mlevphpr* from Bruker library) spectra were recorded using states time proportion phase incrementation for quadrature detection in the indirect dimension. TOCSY spectra run with 4096 × 512 points with a spin lock field of 10 kHz and a mixing time of 60 ms. Chemical shifts displayed relative to external trimethylsilylpropionic acid at 0 ppm for ^{1}H. The data were processed using TopSpin3.1 (Bruker Biospin) (Santos et al. 2015). ^{1}H–^{13}C HSQC spectra run with 1024 × 256 points and globally optimized alternating phase rectangular pulses (GARP) for decoupling ^{1}H–^{13}C HSQC spectra run with 1024 × 256 points and globally optimized alternating phase rectangular pulses (GARP) for decoupling.

Analysis of lability of sulfate esters of fucose units submitted to hydrolysis

Sulfated fucoses (~1 mg) obtained from the FCSs of each species through mild acid hydrolysis and purified by gel filtration (see above) were subjected to further hydrolysis in 0.15 M H_2SO_4 in D_2O. The samples were heated at 100°C at different periods of time (0 → 180 min) and analyzed via 1D ^{1}H NMR spectra as described above.

Mild acid hydrolysis of FCS using DOWEX H^{+}

FCS (20 mg from each species) was dissolved in 2 mL of deionized water and then a suspension DOWEX H^{+} 50w × 8 50–100 mesh (Supelco):deionized water (1:1, v/v) was added up to the solution achieves pH 3. Thereafter, the solutions were centrifuged and the supernatants incubated at 100°C for 45 min, cooled in ice cold, neutralized with 1.0 M NH_4OH and lyophilized. The hydrolysates were analyzed via 1D ^{1}H NMR spectra as described above.

Analysis of disaccharides produced with chondroitin lyase

The oligosaccharides mixture derived from the CS core of FCSs through mild hydrolysis (~1 mg) was incubated with 0.5 unit of

chondroitin ABC lyase (Sigma/Aldrich) in 500 µL of 50 mM Tris–HCl, 5 mM EDTA and 15 mM sodium acetate (pH 8.0). After incubation at 37°C for 12 h, the supernatant containing the released disaccharides was lyophilized and then dissolved in 100 µL of distilled water. The disaccharides derived from FCSs (20 µL) and standard CS disaccharides (Sigma/Aldrich) were analyzed by strong anion-exchange chromatography on a 250 × 5 mm Spherisorb-SAX column (Sigma/Aldrich), linked to a HPLC system (Shimadzu). After sample injection, the column was washed with 5 mL of acidified water (pH 3.5) and the disaccharides eluted from the column using a linear gradient of 0 → 1 M NaCl (pH 3.5) at a flow rate of 1 mL min^{-1} monitored via UV at 232 nm.

ESI-MS and ESI-MS/MS analyses

The hydrolysates were dissolved in 0.05 M ammonium hydroxide and subjected to direct injection analysis at a flow rate of 20 µL min^{-1} on a high-resolution spectrometer quadrupole-Orbitrap Q-Exactive (Thermo Scientific). The mass spectrometer is tuned using an available tuning mix to obtain abundant negative ion(s) of the mass spectrum. The instrument was set to analyse in negative mode with spray voltage 3.8 kV, capillary temperature 380°C, S-lens RF level 80, sheath and auxiliary gas flow rates of 20 and 5 units, respectively and 140,000 of resolution. To ESI-MS we monitoring the 50–500 m/z region of the mass spectra. For the product ions (ESI-MS/MS), we set the interest ion with four of isolation window and use different collision energies (10–50) to obtain the most informative spectra and monitoring the 50–500 m/z region. These conditions for ESI-MS analysis were optimized after testing a variety of parameters and we chose those provoking less degradation of the sample, particularly less desulfation of the compounds.

1D ^{1}H NMR real-time reaction monitoring

FCSs from both species (20 mg of each) were dissolved in 0.5 mL of D_2O, containing 0.5 M HCl in a 5-mm inner diameter NMR tube. The solution was heated at 50°C in the NMR apparatus itself and 1D ^{1}H spectra were recorded at different periods of time (0 → 5 h) as described above.

Supplementary data

Supplementary data is available at *Glycobiology* online.

Acknowledgments

We would like to thank Adriana A Piquet for technical assistance. We also thank the Centro Nacional de Biologia Estrutural e Bioimagem (CENABIO) for the access to the NMR spectrometers.

Funding

This work was supported by grants from Conselho Nacional de Desenvolvimento Cientifico e Tecnológico (CNPq) and Fundação de Amparo à Pesquisa do Estado do Rio de Janeiro (FAPERJ).

Conflict of interest statement

None declared.

References

Bergefall K, Trybala E, Johansson M, Uyama T, Naito S, Yamada S, Kitagawa H, Sugahara K, Bergström T. 2005. Chondroitin sulfate characterized by the E-disaccharide unit is a potent inhibitor of herpes simplex virus infectivity and provides the virus binding sites on gro2C cells. *J Biol Chem*. 280:32193–32199.

Borsig L, Wang L, Cavalcante MC, Cardilo-Reis L, Ferreira PL, Mourão PAS, Esko JD, Pavão MS. 2007. Selectin blocking activity of a fucosylated chondroitin sulfate glycosaminoglycan from sea cucumber. *J Biol Chem*. 282:14984–14991.

Cegelski L. 2015. Bottom-up and top-down solid-state NMR approaches for bacterial biofilm matrix composition. *J Magn Reson*. 253:91–97.

Chen S, Xue C, Yin L, Tang Q, Yu G, Chai W. 2010. Comparison of structures and anticoagulant activities of fucosylated chondroitin sulfates from different sea cucumbers. *Carbohydr Polym*. 83:688–696.

Daniel R, Chevolot L, Carrascal M, Tissot B, Mourão PAS, Abian J. 2007. Electrospray ionization mass spectrometry of oligosaccharides derived from fucoidan of Ascophyllum nodosum. *Carbohydr Res*. 342:826–834.

Fonseca RJC, Oliveira SG, Pomin VH, Mecawi S, Araujo IG, Mourão PAS. 2010. Effects of oversulfated and fucosylated chondroitin sulfates on coagulation. Challenges for the study of anticoagulant polysaccharides. *Thromb Haemost*. 103:994–1004.

Gandhi NS, Mancera RL. 2008. The structure of glycosaminoglycans and their interactions with proteins. *Chem Biol Drug Des*. 72:455–482.

Gao N, Lu F, Xiao C, Yang L, Chen J, Zhou K, Wen D, Li Z, Wu M, Jiang J et al. 2015. β-Eliminative depolymerization of the fucosylated chondroitin sulfate and anticoagulant activities of resulting fragments. *Carbohydr Polym*. 127:427–437.

Huang N, Wu MY, Zheng CB, Zhu L, Zhao JH, Zheng YT. 2013. The depolymerized fucosylated chondroitin sulfate from sea cucumber potently inhibits HIV replication via interfering with virus entry. *Carbohydr Res*. 380:64–69.

Jinno-Oue A, Tanaka A, Shimizu N, Mori T, Sugiura N, Kimata K, Isomura H, Hoshino H. 2013. Inhibitory effect of chondroitin sulfate type E on the binding step of human T-cell leukemia virus type 1. *AIDS Res Hum Retroviruses*. 29:621–629.

Kamba K, Nagata T, Katahira M. 2016. Characterization of the deamination coupled with sliding along DNA of anti-HIV factor APOBEC3G on the basis of the pH-dependence of deamination revealed by real-time NMR monitoring. *Front. Microbiol*. 7:587.

Laezza A, Iadonisi A, Pirozzi AV, Diana P, De Rosa M, Schiraldi C, Parrilli M, Bedini E. 2016. A modular approach to a library of semi-synthetic fucosylated chondroitin sulfate polysaccharides with different sulfation and fucosylation patterns. *Chemistry*. 22:18215–18226.

Li JH, Li S, Zhi ZJ, Yan LF, Ye XQ, Ding T, Yan L, Linhardt RJ, Chen SG. 2016. Depolymerization of fucosylated chondroitin sulfate with a modified fenton-system and anticoagulant activity of the resulting fragments. *Mar Drugs*. 14:e170.

Liu X, Liu Y, Hao J, Zhao X, Lang Y, Fan F, Cai C, Li G, Zhang L, Yu G. 2016a. In vivo anti-cancer mechanism of low-molecular-weight fucosylated chondroitin sulfate (LFCS) from sea cucumber cucumaria frondosa. *Molecules*. 21:e625.

Liu X, Hao J, Shan X, Zhang X, Zhao X, Li Q, Wang X, Cai C, Li G, Yu G. 2016b. Antithrombotic activities of fucosylated chondroitin sulfates and their depolymerized fragments from two sea cucumbers. *Carbohydr Polym*. 152:343–350.

Marques J, Vilanova E, Mourão PAS, Fernàndez-Busquets X. 2016. Marine organism sulfated polysaccharides exhibiting significant antimalarial activity and inhibition of red blood cell invasion by Plasmodium. *Sci Rep*. 6:24368.

Melo-Filho NM, Belmiro CL, Gonçalves RG, Takiya CM, Leite M, Pavão MSG, Mourão PAS. 2010. Fucosylated chondroitin sulfate attenuates renal fibrosis in animals submitted to unilateral ureteral obstruction: A P-selectin-mediated event? *Am J Physiol Renal Physiol*. 299: 1299–1307.

Mourão PAS, Pereira MS, Pavão MS, Mulloy B, Tollefsen DM, Mowinckel MC, Abildgaard U. 1996. Structure and anticoagulant activity of a

fucosylated chondroitin sulfate from echinoderm. Sulfated fucose branches on the polysaccharide account for its high anticoagulant action. *J Biol Chem*. 271:23973–23984.

Myron P, Siddiquee S, Al Azad S. 2014. Fucosylated chondroitin sulfate diversity in sea cucumbers: A review. *Carbohydr Polym*. 112:173–178.

Neville GA, Mori F, Holme KR, Perlin AS. 1989. Monitoring the purity of pharmaceutical heparin preparations by high-field 1H-nuclear magnetic resonance spectroscopy. *J Pharm Sci*. 78:101–104.

Panagos CG, Thomson DS, Moss C, Hughes AD, Kelly MS, Liu Y, Chai W, Venkatasamy R, Spina D, Page CP et al. 2014. Fucosylated chondroitin sulfates from the body wall of the sea cucumber Holothuria forskali: Conformation, selectin binding, and biological activity. *J Biol Chem*. 289: 28284–28298.

Pomin VH, Pereira MS, Valente AP, Tollefsen DM, Pavão MS, Mourão PAS. 2005a. Selective cleavage and anticoagulant activity of a sulfated fucan: Stereospecific removal of a 2-sulfate ester from the polysaccharide by mild acid hydrolysis, preparation of oligosaccharides, and heparin cofactor II-dependent anticoagulant activity. *Glycobiology*. 15:369–381.

Pomin VH, Valente AP, Pereira MS, Mourão PAS. 2005b. Mild acid hydrolysis of sulfated fucans: A selective 2-desulfation reaction and an alternative approach for preparing tailored sulfated oligosaccharides. *Glycobiology*. 15:1376–1385.

Queiroz IN, Wang X, Glushka JN, Santos GR, Valente AP, Prestegard JH, Woods RJ, Mourão PA, Pomin VH. 2015. Impact of sulfation pattern on the conformation and dynamics of sulfated fucan oligosaccharides as revealed by NMR and MD. *Glycobiology*. 25:535–547.

Santos GRC, Glauser BF, Parreiras LA, Vilanova E, Mourão PAS. 2015. Distinct structures of the α-fucose branches in fucosylated chondroitin sulfates do not affect their anticoagulant activity. *Glycobiology*. 10:1043–1052.

Sugahara K, Tanaka Y, Yamada S. 1996. Preparation of a series of sulfated tetrasaccharides from shark cartilage chondroitin sulfate D using testicular hyaluronidase and structure determination by 500 MHz 1H NMR spectroscopy. *Glycoconj J*. 13:609–619.

Vieira RP, Mourão PAS. 1988. Occurrence of a unique fucose-branched chondroitin sulfate in the body wall of a sea cucumber. *J Biol Chem*. 34: 18176–18183.

Vilanova E, Santos GR, Aquino RS, Valle-Delgado JJ, Anselmetti D, Fernàndez-Busquets X, Mourão PAS. 2016. Carbohydrate-carbohydrate interactions mediated by sulfate esters and calcium provide the cell adhesion required for the emergence of early metazoans. *J Biol Chem*. 291: 9425–9437.

Vinnitskiy DZ, Ustyuzhanina NE, Dmitrenok AS, Shashkov AS, Nifantiev NE. 2017. Synthesis and NMR analysis of model compounds related to fucosylated chondroitin sulfates: GalNAc and Fuc(1 → 6)GalNAc derivatives. *Carbohydr Res*. 438:9–17.

Wu N, Ye X, Guo X, Liao N, Yin X, Hu Y, Sun Y, Liu D, Chen S. 2013. Depolymerization of fucosylated chondroitin sulfate from sea cucumber, Pearsonothuria graeffei, via 60Co irradiation. *Carbohydr Polym*. 93: 604–614.

Yang J, Wang Y, Jiang T, Lv L, Zhang B, Lv Z. 2015. Depolymerized glycosaminoglycan and its anticoagulant activities from sea cucumber Apostichopus japonicus. *Int J Biol Macromol*. 72:699–705.